Macropinocytosis of human papillomaviruses in natural killer cells via CD16 induces cytotoxic granule exocytosis and cytokine secretion.[1]

Virginie Renoux[*], Inge Langers[*], Bettina Bisig[*], Estelle Dortu[*], Béatrice Clémenceau[†], Marc Thiry[‡], Christophe Deroanne[§], Alain Colige[§], Jacques Boniver[*], Philippe Delvenne[*] and Nathalie Jacobs[*]

[*] Laboratory of Experimental Pathology, GIGA-I3, University of Liège, B23/4, Sart Tilman, 4000 Liège, Belgium
[†] INSERM U892, Institut de Recherche thérapeutique de l'Université de Nantes, Nantes, France,
[‡] Cellular and Tissular Biology, GIGA-Neurosciences, University of Liège, L3, 4000 Liège, Belgium
[§] Laboratory of Connective Tissues Biology, GIGA-Cancer, University of Liège B23/3, Sart Tilman, 4000 Liège, Belgium

Running title: HPV-VLP induce NK cell degranulation and cytokine production**.**

Corresponding Author:
Nathalie Jacobs
Phone: +3243662420
Fax: +3243669583
Email: n.jacobs@ulg.ac.be

Abbreviations:

DC: dendritic cell; HPV: human papillomavirus; PBMC: peripheral blood mononuclear cell; SCC: squamous cell carcinoma; SIL: squamous intraepithelial lesion; VLP: virus-like particles; WT: wild type.

Keywords:
NK cells, viral infection, Fc receptors, vaccination, Tumor immunity

[1] This study was supported by the Belgian National Fund for Scientific Research (FNRS). NJ CD and AC are supported by the FNRS. VR, BB and IL are supported by a Télévie grant from the FNRS.

Abstract

Persistent infection with oncogenic human papillomavirus (HPV) genotypes is a necessary cause of anogenital cancer. Although infection of basal keratinocytes is well documented, it remains unclear whether virions can also specifically target other cell types such as immune cells for uptake and adsorption. Moreover, it is known that HPV virus-like particles (VLP), the prophylactic vaccine against HPV-associated cervical cancer, are able to activate dendritic cells (DC). However, no study has been performed with other innate cells such as Natural Killer (NK) cells. In the present study, we showed, by flow cytometry and by confocal and electron microscopy that NK cells internalize HPV-VLP. We also demonstrated that virus entry into NK cells is mediated by macropinocytosis and is independent of clathrin and caveolin pathways. In order to test whether NK cell activity is influenced by HPV, we also studied lytic granule exocytosis and cytokine secretion. We observed an increased cell degranulation and a higher TNF-α and IFN-γ secretion in the presence of HPV-VLP. Moreover, we showed that CD16 expression plays a key role both in viral adsorption and in subsequent NK cytotoxic degranulation and cytokine production.

In conclusion, our data indicate for the first time that HPV interacts with NK cells and activates them.

Introduction

High-risk human papillomaviruses (HPV) are causative agents of uterine cervical cancer (1) and have also been etiologically associated with other anogenital tumors (2, 3) and with head and neck carcinomas (4). Among the 100 HPV genotypes already characterized, 15 are implicated in uterine cervical cancer and more than 50% of these lesions are associated with HPV16 (5). Because of their keratinocyte differentiation-dependent life cycle, virus production *in vitro* has required complex cell culture systems and only low virus titers can be obtained (6). Consequently, most studies aiming to investigate virus interactions with host cells have used virus-like particles (VLP), which result from self-assembly HPV L1 major capsid proteins and which are morphologically and immunologically similar to native virions (7-9). Moreover, two HPV L1 VLP prophylactic vaccines have recently been licensed (10, 11).

HPV-VLP are able to enter into keratinocytes (12-14), the natural host of HPV infection, but also into immune cells such as antigen-presenting cells (15). Interestingly, VLP internalization in dendritic cells (DC) induces their maturation and promotes a cell-mediated immune response against HPV (9, 16). The potential interaction of HPV with other immune cells is still poorly studied. We therefore investigated whether HPV-VLP modulate the activity of Natural Killer (NK) cells, which play a major role in anti-viral (17, 18) and anti-tumoral responses (19).

Classically, NK cells are defined as a CD3- CD16+ CD56+ lymphocyte subpopulation but recently, NKp46 has been described as a specific marker for the detection of both human and mouse NK cells (20). These cells play an important role in the early phase of immune responses against viruses and tumors by exhibiting cytotoxic functions and secreting a number of cytokines (21, 22). Cytotoxic activity of NK cells is mediated by exocytosis of preformed cytotoxic granules containing perforin and granzymes (23, 24). Binding of

antibodies onto CD16, a low affinity receptor for the fragment crystallizable (Fc) region of IgG (FcγRIII) highly expressed by NK cells (25), induces Antibody-Dependent Cellular Cytotoxicity (ADCC) (26). Interestingly, FcγRII/III have been described as being involved in HPV-VLP internalization in DC (27). Besides their cytotoxic activity, NK cells indirectly activate a cell-mediated immune response by secretion of IFN-γ and TNF-α (28). NK cells are mainly found in the peripheral blood, but they are also present in several lymphoid (29) and non-lymphoid tissues, for example in the uterine mucosa (30). NK cells are able to recognize viral capsids, since filovirus-derived VLP directly activate NK cells (31). Moreover, increased numbers of CD56+ cells have been observed in HPV-associated preneoplastic lesions (32). These results suggest that HPV could also interact with NK cells.

In this study, we investigated the interactions between NK cells and HPV-VLP. We first observed an infiltration of NKp46+ NK cells in HPV associated-preneoplastic lesions. We also demonstrated by flow cytometry as well as confocal and electron microscopy that HPV-VLP enter rapidly into blood NK cells. Using inhibitory drugs, we demonstrated that HPV-VLP entry is independent of clathrin and caveolin pathways but is mediated by macropinocytosis. The uptake of extracellular fluid and activation of the RhoGTPase Cdc42 confirmed the involvement of the macropinocytosis pathway. Entry of HPV-VLP did not occur into the NK92 cell line, a CD16 negative NK cell line and transduction of CD16 in NK92 cells restored HPV-VLP entry, suggesting a role for CD16 in HPV-VLP uptake in NK cells. Furthermore, we demonstrated that HPV-VLP induce CD16-dependent cytotoxic granule exocytosis and cytokine secretion by NK cells.

Material and methods

Cell lines and primary cells

CasKi cell line was obtained from ATCC and grown in DMEM (GIBCO, Merelbeke, Belgium) medium supplemented with 10% FBS (GIBCO), and 1% Pyruvate sodium (GIBCO), 1% non essential amino acids (GIBCO).

The NK cell line, NK92 (33), was transduced with CD16 using the lentiviral system as previously described (34). In order to increase the level of CD16 expression, NK92 cells expressing a high level of CD16 were sorted by flow cytometry. NK92 CD16+ and parental cell lines were grown in RPMI 1640 medium (GIBCO) supplemented with 8% human serum (centre de transfusion sanguine, Centre Hospitalier Universitaire, Liège, Belgium) and 100 IU/ml of IL2 (Proleukine, Novartis, Vilvoorde, Belgium).

NK cells were isolated from peripheral blood mononuclear cells (PBMC) obtained from buffy coat of healthy donors (Centre de transfusion sanguine de Liège, Belgium). Briefly, diluted blood was slowly deposited on Lymphoprep (Lucron Bioproducts, Sint-Martens-Latem, Belgium) and after 30 min of centrifugation, PBMC were collected. After 3 washes in RPMI medium, cells were incubated for 10 min at room temperature with a human NK cell enrichment cocktail (EasySep® Human NK Cell Enrichment Kit, STEMCELL technologies, Grenoble, France) followed by incubation with EasySep® magnetic particles for 5 min. After negative sorting, the purity of NK cells was assessed by flow cytometry and the percentage of NK cells (CD56+CD16+CD3-) was > 95%.

DC were obtained after a seven-day culture of CD14+ monocytes in complete RPMI 1640 with 800 U/ml human recombinant GM-CSF and 40 U/ml IL-4 (ImmunoTools, Friesoythe, Germany). Monocytes are obtained by a CD14-positive selection of PBMC using a MACS system (Miltenyi, Utrecht, the Netherlands).

All cells were cultivated in a humidified incubator at 37°C in 5% CO_2 in medium supplemented with 50 IU/ml of penicillin (GIBCO) and 50 µg/ml of streptomycin (GIBCO). This study was approved by the Ethics Committee of the University Hospital of Liège.

Immunostaining of NK cells

The density of NK cells was assessed by immunohistochemistry in formalin-fixed paraffin-embedded cervical tissue samples, derived from biopsies or surgical specimens of 39 patients. These comprised 69 mucosal regions representative of 4 different histopathological categories, including 20 normal exocervical mucosae, 9 normal endocervical mucosae, 26 squamous intraepithelial lesions (SIL, both high grade and low grade) and 14 invasive squamous cell carcinomas (SCC).

After antigen retrieval, performed by pressure cooking for 6 min in citrate buffer (pH 6), 4 µm-thick tissue sections were incubated overnight with a mouse monoclonal antibody directed against NKp46/NCR1 (clone 195314, R&D Systems, Oxon, UK) at a dilution of 1/100. Immunoperoxidase detection was performed using the LSAB2 kit and the 3,3′-diaminobenzidine (DAB) substrate (Dako, Glostrup, Denmark). Sections were counterstained with haematoxylin. The number of cells stained with the anti-NKp46 antibody was counted in 10 adjacent high power fields per sample. The epithelial and stromal components were assessed separately.

The purity of NK cells and the modulation of receptors on their surface were assessed by flow cytometry. The following antibodies were used: CD3-PerCP, CD56-PE, CD16-HorizonV450, CD14-FITC (BD Biosciences, Erembodegem, Belgium) and NKp46-APC (Miltenyi). All experiments were analyzed with FACS Canto II and Diva software (Becton Dickinson).

Production and purification of HPV16 and HPV31 VLP

HPV16 and HPV31 VLP were generated in Sf9 insect cells by co-infection with recombinant baculoviruses carrying the L1 gene of HPV16 or HPV31, kindly provided by P Coursaget and purified as described in (35). The presence of L1 protein was analyzed by SDS-PAGE gels and quantified after resuspension in NaCl 0.15 M by a BCA dosage (Thermo Fisher, Tournai, Belgium). An ELISA with the conformational H16.V5 mAb (36) was performed to control the conformation of VLP HPV16.

Labeling of HPV-VLP with CFDA-SE

Purified HPV16 or HPV31 VLP were diluted with PBS (pH 8.5) to a concentration of 0.5 mg/ml. Carboxy-fluorescein diacetate succinimyl ester **(**CFDA-SE, Invitrogen, Merelbeke, Belgium), resuspended in DMSO, was added to the final concentration of 100 µM (37). After 16h of incubation at room temperature in the dark, the mixture was centrifuged (6 h at 28 000 r.p.m in a SW28 rotor, Beckman-Coulter, Suarlee, Belgium) on a 30% and 70% sucrose density gradient to separate coupled VLP from free CFDA-SE. Under these conditions, CFDA-SE remains on the top of the gradient as visualized by fluorescent CFSE, which is formed due to spontaneous decay in aqueous solutions. VLP labeled with CFDA-SE were resuspended in 0.15 M NaCl and then analyzed by SDS-PAGE and protein quantification by BCA dosage.

CFDA-SE-VLP entry

To follow the entry of VLP into NK cells, 2.10^5 cells were incubated for 1h at 4 °C with 10 µg of CFDA-SE-VLP in 200 µl of complete RPMI to allow the binding of VLP onto the cell surface. After a wash with 1 ml of medium, supernatant was removed and cells were resuspended in 200 µl of complete medium and placed in an incubator (37 °C, 5% CO_2). Cells were centrifuged and pellets were resuspended in 300 µl of 1% paraformaldehyde (PAF).

Different drugs were used to determine the entry pathway: 2 µM of cytochalasin D (disruption of actin filaments and inhibition of actin polymerization, Sigma), 25 µg/ml of chlorpromazine (dissociation of clathrin lattice, Sigma) for the clathrin-dependent pathway and 25 µg/ml of nystatin (disruption of the cholesterol-enriched caveola-containing membrane microdomain, Sigma) for the caveolae-dependent pathway. Drugs were added to the medium containing NK cells 1h before the beginning of the kinetic. To determine whether the structure of VLP was necessary for VLP entry, we destroyed this structure by heating at 95 °C for 30 min. To examine the role of heparan sulfates in cell binding, NK cells were also incubated with heparinase II (1 U/ml, Sigma), which cleaves a-N-acetyl-D-glucosaminidic linkage. After incubation for 1 h at 37 °C and one wash with PBS, NK cells were incubated with labeled VLP.

Confocal microscopy

After incubation with HPV16-VLP, NK cells, NK92 CD16+ and CD16- cells (5.10^5 in 300 µl of complete medium) were incubated for 1 hour with Hoechst 33342 (10 µM, Acros Organics, Geel, Belgium). After one wash, cells were deposited on a coverslip (diameter: 12 mm, VWR) coated with polylysin (Sigma) for 15 minutes. The supernatant was withdrawn, cells were fixed for 20 minutes with PAF (4%) and the cell membrane was stained with phalloidin 633 (Invitrogen) for 45 min at room temperature in the dark. After one wash, the coverslip was dried with absolute ethanol and fixed with 20 µl of Mowiol (Hoechst GmbH, Frankfurt, Germany). Images were acquired using an Olympus Fluoview FV1000 confocal system (Olympus, Aartselaar, Belgium) equipped with an Olympus IX81 inverted microscope (objective UPLSAPO 60X / NA 1.35).

Transmission electron microscopy

To check VLP conformation, 10 µl of each VLP pool were deposited on copper grids coated with a carbon film (EMS, Brussels, Belgium) for 1 min. Excess of VLP was removed and grids were strained twice with 2% uranyl acetate (Fluka, Bornem, Belgium) for 1 min. Grids were washed with filtered demineralized water and were observed with a transmission electron microscope LEO 906E (60 kV) (Zeiss, Zaventem, Belgium).

To analyze VLP entry, NK cells were incubated with VLP as described above for different lengths of time (10 min to 18 h). Cells were then centrifuged at room temperature, fixed at room temperature in 4% glutaraldehyde (Laborimpex, Brussels, Belgium) and post-fixed in 1% osmium tetroxide (Laborimpex) for 1 h at 4 °C. Cells were then dehydrated in graded (70, 90, 100%) ethanol solutions (VWR International, Leuven, Belgium). Fixed cells were embedded in Epon (Serva, Breda, the Netherlands) and propylene oxide (Laborimpex), and hardened at 60 °C. Ultrathin sections were stained with uranyl acetate (Fluka) and lead citrate (Leica, Groot Bijgaarden, Belgium). These sections were examined using a transmission electron microscope EM Jeol 100 CX II (Jeol, Zaventem, Belgium).

Extracellular fluid uptake

A fluid-uptake assay with FITC-Dextran was performed on negatively sorted NK cells and NK92 cell lines. The cells (2.10^5) were cultured in 200 µl of complete RPMI containing 1 mg/ml of FITC-Dextran (average mol wt 20,000, Sigma). Ten µg/ml of HPV16-VLP, 1 µg/ml of extract of Sf9 nucleus infected by wild-type baculovirus, 10 µg/ml of disrupted HPV16-VLP or 5 µg/ml of purified CD16 antibody (BD Biosciences) were added for 10 minutes or 1 hour at 37 °C. After incubation, cells were washed 3 times and fixed (PAF 1%). Cells treated with 2 µM of cytochalasin D (Sigma) for 30 minutes before the incubation of HPV-VLP were also used as controls.

Assay for activated GTPase protein detection

The assay to detect activated GTPase proteins was carried out as previously described (38) with some modifications. Briefly, cells in suspension in 200 µl of culture medium were lysed by addition of 200 µl of ice-cold buffer containing 1% Triton X-100, 50 mM Hepes, pH 7.3, 150 mM NaCl, 8% glycerol, 40 mM β-glycerophosphate, 0.2 mM 4-(2-aminoethyl)benzenesulfonyl fluoride, and 8 µg/ml aprotinin. Lysates were centrifuged for 5 min at 16,000×*g*. Supernatants were immediately frozen in liquid nitrogen and stored at -80 °C until use. An aliquot of each supernatant collected before freezing was denatured in SDS-PAGE lysis buffer to measure the total RhoGTPase content by Western blotting. For pull-down assays, supernatants were incubated for 30 min with 30 µg of GST-PBD protein containing the Cdc42 and Rac binding region of PAK-1B, affinity linked to glutathione-Sepharose beads. The beads were washed 4 times in ice-cold buffer containing 0.5% Triton X-100, 25 mM Hepes (pH 7.3), 150 mM NaCl, 4% glycerol, 10 mM NaF, 20 mM β-glycerophosphate, 0.1 mM 4-(2-aminoethyl)benzenesulfonyl fluoride, 4 µg/ml aprotinin and boiled in 60 µl of SDS-PAGE lysis buffer. The amount of Rac1 and Cdc42 in the samples was determined by immunoblotting with antibodies specific to Rac1 (mouse anti-Rac1 (23A8) from Upstate Biotechnology, Waltham, USA) and Cdc42 (mouse anti-Cdc42 from BD Biosciences).

Degranulation assay

To measure degranulation on NK or NK92 cells, 2.10^5 cells were cultured in 200 µl of complete RPMI medium in 96-well plates alone, with 1 µg/ml of HPV16-VLP, using purified CD16 antibody (BD Biosciences) at a concentration of 5 µg/ml, or with Phorbol 12-myristate 13-acetate (PMA)/ionomycine, 10 ng/ml and 1 µg/ml, respectively (Calbiochem, Nottingham, United Kingdom) used as positive controls. One µg/ml of extract of Sf9 nucleus infected by wild-type baculovirus was used as negative controls. The NK cells cultured in medium only

were taken as a measure of "spontaneous" NK cell degranulation. After one or six hours, cells were centrifuged, resuspended in 20 µl of PBS supplemented with 0.5% of FBS and incubated for 1 h with 5 µl of CD107a-PE (BD Biosciences) on ice. CD107 expression on the cell surface was a measurement of the degranulation of intracellular lytic vesicles by NK cells. Samples were washed with PBS-0.5% FBS, centrifuged and fixed in 300 µl of paraformaldehyde (PAF) 1%.

ELISA

To quantify TNF-α and IFN-γ secretion, 1.10^6 of NK or NK92 cells were placed in 1 ml of complete RPMI medium in 24-well plates alone, with 1 µg of HPV16-VLP, with purified CD16 antibody (5 µg/ml, BD Biosciences) or PMA/ionomycine (10 ng/ml and 1 µg/ml, respectively; Calbiochem) used as positive controls, or with 1 µg of extract of Sf9 nucleus infected by wild-type baculovirus, used as negative controls. Culture supernatants were stored at -80 °C and were analyzed for TNF-α and IFN-γ production in a specific capture ELISA according to the manufacturer's instructions (Biosoure, Merelbeke, Belgium).

Statistics

Prism 4.0 (GraphPad Software) was used for data handling, analysis and graphic representation. Statistical analysis was performed using the Student's *t* test or the Mann Whitney test.

Results

NKp46+ cells are present in cervical squamous intraepithelial lesions (SIL)

In order to determine whether NK cells are present in normal cervical mucosa and lesions, we performed NKp46 immunostaining on tissue samples (Fig. 1). Because more than 85% of HPV-associated cervical lesions occur in the region of the junction between the endocervix and exocervix (39), we chose these tissues as normal controls. NK cells were mainly observed in the subepithelial stroma of normal endocervix, exocervix, SIL and SCC (Fig. 1*A*-*E*) and the number of NK cells was increased in the peritumoral stroma of SCC cases ($p<0.05$) (Fig. 1*D*-*E*). The quantification of NK cells in the epithelium (Fig. 1*F*) showed a significant infiltration of NKp46+ cells in SIL compared to normal epithelium, but not in SCC despite the presence of more numerous NK cells in the surrounding stroma. Interestingly, virus particles have been detected mainly in SIL and not in SCC (40, 41) where the virus is usually integrated into the host genome (42). Our results thus suggest that NK cells could interact with virus particles.

HPV-VLP are internalized in NK cells

We first studied the possible HPV-VLP internalization in NK cells using CFDA-SE-labeled VLP. CFDA-SE is a marker, that becomes fluorescent inside the cells only after the removal of the acetate groups by cellular serine esterase (37). We performed a kinetic study with HPV16-VLP-CFDA-SE at 37 °C on NK cells negatively selected from blood (Fig. 2*A*). The epithelial cell line, CasKi, was used as a positive control (14) and showed a peak of fluorescence after 24 h, whereas the fluorescence observed for NK cells was weaker, but reached a plateau very quickly (after 10 min) (Fig. 2*A*). HPV-VLP internalization has been previously described in DC (15, 27) and here we compared the entry into DC and NK cells derived from the same donor. After 10 min of incubation, we observed a higher fluorescence in NK cells compared to DC (Fig. 2*B*). This uptake was not restricted to VLP from HPV16, since the VLP entry into NK cells was similar with HPV31-VLP and HPV16-VLP (Fig. 2*C*).

HPV-VLP internalization was HPV-VLP dose dependent (Supplementary file S1A) and CFDA-SE-VLP fluorescence in NK cells was inhibited by incubation with an excess of uncoupled VLP (Supplementary file S1B).

The HPV-VLP entry seemed to require an active process because entry did not occur at 4 °C (Fig. 2*D*), whereas fluorescence of CFDA-SE after cellular uptake without VLP was not affected at 4 °C (data not shown). This showed that the absence of CFDA-SE fluorescence was not due to the absence of intracellular enzyme cleavage at 4° C. When the VLP structure was disrupted by heating at 95 °C, the resulting fluorescence intensity in NK cells was significantly decreased, suggesting that the conformation of VLP is important for the process of internalization (Fig. 2*D*). The inhibition of fluorescence was not related to heat degradation of CFDA-SE because heating the CFDA-SE at 95 °C before VLP labeling inhibited its fluorescence marginally (data not shown).

In order to visualize the entry of VLP into NK cells, we performed confocal microscopy analyses (Fig. 3). We detected fluorescent HPV-VLP localized in a few large fluorescence spots inside NK cells as early as 10 min of VLP incubation at 37 °C (Fig. 3*A*) but not in DC or in CasKi cells (data not shown). After 5 h of incubation, HPV-VLP were observed as being dispersed into the cytoplasm of DC (Fig. 3*B*) and of CasKi cells (Fig. 3*C*). This HPV-VLP distribution was not observed in NK cells even after a longer incubation time.

To further confirm these results, electron microscopy experiments were performed on sorted NK cells incubated with HPV16-VLP (Fig. 4). Figure 4A shows an internalization of HPV-VLP in large vacuoles (mean diameter: 0.24 ± 0.14 µm, n=22) after 10 min of incubation. Similar observations were made after 6, 12 and 18 hours and fusion of these vacuoles with the nucleus was not observed (data not shown). At later incubation time, 18 hours, we noticed very large vacuole, which could come from fusion of smaller vesicles. In this large vacuole the HPV-VLP seemed partially degraded (Fig. 4*B*). We did not observe clathrin-coated

vesicles containing HPV-VLP in NK cells as observed in DC (Fig. 4*C*) where the vacuole size was smaller (mean diameter: 0.12 ± 0.3 µm, n=6).

HPV16-VLP uptake in NK cells is mediated by macropinocytosis

The membrane ruffles observed by electron microscopy on NK cells in the presence of HPV-VLP (Fig. 4*D-E*) suggested a macropinocytosis mechanism for HPV-VLP endocytosis. In addition to cell surface ruffling, macropinocytosis is characterized by the uptake of extracellular fluid and by activation of RhoGTPases (43). To confirm this mechanism of endocytosis, we carried out fluid uptake assays with FITC-Dextran (Fig. 5*A*). In the presence of HPV-VLP, the fluorescence had already increased in NK cells at 10 min and increased further at 1 h (Fig. 5*A*, black squares). This increase was significantly inhibited by cytochalasin D (Fig. 5*A*, white squares), the most commonly used agent to block macropinocytosis (44). As a negative control, we used cell lysate from insect cells infected with wild-type baculovirus (WT condition) instead of a baculovirus containing the L1 gene, and no significant increase in fluorescence was observed (Fig. 5*A*, black triangles). The destruction of the VLP structure by heating at 95 °C impaired extracellular fluid uptake (Fig. 5*A*, black circles). In order to further characterize the macropinocytosis mechanism, we tested, using GTPase assay, the activity of two RhoGTPases, Cdc42 and Rac1, which have been described as playing a role in the entry of many viruses into host cells (43). These results indicated that HPV-VLP induced a rapid activation of Cdc42 (Fig. 5*B*) and an inhibition of Rac1 in NK cells (Fig. 5*B*).

Since the role of the caveola and clathrin pathways has previously been described for HPV entry (45, 46) we tested their involvement in HPV-VLP internalization in NK cells with drugs inhibiting caveolin (nystatin) or clathrin (chlorpromazine) vacuole formation (Fig. 5*C*). The absence of a significant inhibition of HPV-VLP entry after 10 min or 3 h of incubation with these drugs (Fig. 5*C*) suggested that these pathways were not used in NK cells, whereas

cytochalasin D, a drug that blocks macropinocytosis, inhibited HPV-VLP entry (Fig. 5*C*). Effectiveness of chlorpromazin and nystatin was tested on DC in the presence of HPV-VLP (15).

CD16 is required for rapid HPV16-VLP uptake in NK cells

Interactions with heparan sulfates have been described as an initial step for HPV-VLP entry into keratinocytes (47), but also into immune cells such as DC (15). We studied the involvement of heparan sulfate using heparinase II and showed that this enzyme inhibited partially HPV-VLP entry into NK cells (supplementary file S2).

We also investigated the role of CD16 in HPV-VLP entry because we observed a very low HPV-VLP uptake in an NK cell line (NK92), which does not express CD16 (supplementary file S3). Moreover, CD16 has been reported to be involved in HPV-VLP binding onto DC (8). Interestingly, CD16 transduction in the NK92 cell line partially restored the uptake of CFDA-SE labeled HPV-VLP (referred as NK92 CD16+/-, Fig. 6*A*-*B*). The level of CD16 in these cells was low (ratio of mean fluorescence 10 ± 2 compared to 98 ± 9 for NK purified from blood). To increase the level of CD16, the NK92 cells expressing the highest level of CD16 were sorted by flow cytometry. These cells, referred to as NK92 CD16+, had a CD16 ratio of mean fluorescence of 28 ± 2 and showed a better internalization of HPV-VLP after 10 min (Fig. 6*A*) and 3 h (Fig. 6*B*) of incubation. For the following experiments, we used these NK92 CD16+ sorted cells. We confirmed HPV-VLP entry in NK92 CD16+ cells by confocal (Fig. 6*C*) and electron microscopy (data not shown). Similar pictures were obtained for NK92 CD16+ cells (Fig. 6*C*) and for blood sorted NK cells (Fig. 3*A*). In NK92 CD16- cells, we were not able to detect any fluorescence inside the cells after 10 min (Fig. 6*D*).

To determine whether macropinocytosis was also involved in HPV-VLP entry into the NK92 CD16+ cells, we carried out an FITC-dextran uptake assay. We observed an increase in FITC fluorescence in NK92 CD16+ cells in the presence of HPV-VLP (Fig. 6*E*, black squares),

whereas no fluid uptake was detected in the NK92 CD16- cells (Fig. 6*F*). The conformation of VLP also seemed necessary for HPV-VLP entry, since the destruction of VLP by heating abolished fluid uptake (Fig. 6*E*, black circles).

To further study the role of CD16 in HPV-VLP internalization, we analyzed the surface expression of CD16 on cell surface of NK cells and NK92 CD16+ cell line in the presence of HPV-VLP (Fig. 7). We observed a transient down-modulation of CD16 cell surface expression in both cell types (Fig. 7*A*-*B*), but the kinetic was faster in NK cells (Fig. 7*A*) compared to NK92 CD16+ cells (Fig. 7*B*). As a control, we analyzed the expression of another NK receptor, NKp46, and we did not observe any significant change in cell surface expression of NKp46 on NK cells (Fig. 7*C*).

HPV-VLP induce degranulation of NK cells

In order to determine whether the interactions between NK cells and HPV-VLP could modify the cytotoxic activity of NK cells, we analyzed the exocytosis of cytotoxic granules of NK cells in the presence of HPV-VLP by measuring the expression of lysosomal-associated membrane protein 1 (CD107a) on the NK cell surface. CD107a expression correlates with cell cytotoxicity activity (48). PMA/ionophore or anti CD16 mAb were used as positive controls (49). As shown in Figure 8, lysate of insect cells infected with WT baculovirus (WT condition) did not induce an increase in CD107a positive cells, whereas HPV-VLP significantly increased the number of CD107a positive NK cells after 10 min (data not shown), 1 h or 6 h of incubation (Fig. 8*A*). Degranulation was also observed in NK92 CD16+ cells in the presence of HPV-VLP (Fig. 8*B*). In the absence of CD16, NK92 cells were not able to degranulate in the presence of HPV-VLP; however these cells did degranulate in the presence of PMA/ionophore (Fig. 8*C*).

HPV-VLP induce TNF-α and IFN-γ secretion

In addition to their capacity to exhibit cytotoxic activity, NK cells are also able to secrete cytokines to promote cell-mediated immune responses. Consequently, we measured the production of TNF-α and IFN-γ after 6 h (Fig. 9) or 24 h (data not shown) of culture in the presence of HPV-VLP. NK cells incubated with HPV-VLP secreted significantly more TNF-α (Fig. 9*A*) and IFN-γ (Fig. 9*B*) compared to cells without VLP. This cytokine production was not due to insect cell or baculovirus contaminants, since we did not observe significant amount of cytokines in our negative control (Fig. 9). The structural integrity of VLP is required for cytokine secretion, since heating disruption of VLP decreased TNF-α (Fig. 9*A*) and IFN-γ (Fig. 9*B*) production. Similar cytokine production was observed with NK92 CD16+ in the presence of HPV-VLP (Fig. 9). No TNF-α or IFN-γ were produced by NK92 CD16- cells (data not shown), but these cells were able to secrete large amounts of these cytokines in the presence of PMA/ionophore (1708 ± 345 pg/ml for TNF-α and 3086 ± 998 pg/ml for IFN-γ).

Discussion

Understanding interactions between HPV and immune cells is important in order to dissect the mechanisms responsible for viral clearance observed in the majority of patients with SIL (50). Moreover, the immune response against HPV induced by HPV-VLP vaccination is poorly characterized. In this study, we demonstrated that NK cells recognize, internalize and respond to HPV-VLP by cytotoxic granule exocytosis and cytokine production. Da Silva et al. (2001) reported a weak binding of HPV-VLP in a single study on NK cells and HPV-VLP (8). This weak detection of HPV-VLP on the cell surface could be explained by the rapid entry of HPV-VLP into NK cells (Fig. 2). Interestingly, a more recent study from the same authors highlighted the importance of low-affinity FcγR such as CD16 for HPV-VLP uptake in a mouse model (27).

In order to investigate whether NK cells could interact with HPV *in vivo*, we studied the presence of NK cells in tissue samples with NKp46 immunostaining (Fig. 1). We observed that NK cells infiltrate mainly HPV-associated preneoplastic lesions where HPV particles can be produced, but less SCC where the expression of L1 protein is not detected (41). These findings confirmed the data of Kobayashi and colleagues using a less specific marker for NK cells, CD56, and showing an increased number of CD56+ cells in HPV-related preneoplastic lesions (32). Moreover, NK cells may also interact with HPV-VLP used as a prophylactic anti-HPV vaccine (11), since the adjuvant present in the vaccine induces local inflammation (51), and since infiltration of NK cells has been observed in inflamed tissues (52, 53).

The mechanism of HPV-VLP entry has been widely described for keratinocytes (54, 55), DC and Langerhans cells (15). HPV-VLP have been shown to enter into these cells within small endocytosis clathrin- or caveolin-coated vesicles (45, 56). Interestingly, in the present study, the HPV-VLP internalization mechanism was observed to be different for NK cells, where HPV-VLP entry occurred within large macropinocytosis vacuoles independently of clathrin and caveolae pathways (Fig. 4-5). Moreover, the entry was faster into NK cells compared to

keratinocytes or DC. This rapid internalization has also been observed in Langerhans cells (15). The activation of the RhoGTPase, Cd42, with inhibition of Rac1 activation during HPV-VLP uptake suggests the involvement of filopodia formation (57, 58) and not membrane blebbing, as described for vaccinia or dengue virus host-cell entry (59, 60). These filopodia were observed by electron microscopy (Fig. 4*D-E*).

Heparan sulfates have been described as initial attachment receptors for HPV-VLP (15, 47). In the present study, heparinase II partially inhibited HPV-VLP entry into NK cells (supplementary file S2). However, our results suggest that HPV-VLP uptake in NK cells is dependent on CD16 expression. The HPV-VLP internalization induced transient down-modulation of CD16 (Fig. 7) and the entry into NK92 cells transduced with CD16 was correlated with the level of CD16 expression (Fig. 6*A*). Our findings are in agreement with those of Da Silva and colleagues, who showed that binding of HPV-VLP is mediated by CD16 on DC (8) and that uptake of HPV-VLP by DC from FcγRII/III-deficient mice is strongly reduced compared with wild-type mice (27). Moreover, we observed no induction of macropinocytosis in NK92 CD16- (Fig. 6*F*). CD16 has been shown to be involved in macropinocytosis in macrophages (61) and, more recently, in γδ T cells (62). Other NK receptors do not seem to be involved. For example, we did not observe a down-modulation of NKp46, a receptor involved in Newcastle disease virus binding (63) (Fig. 7*C*), and transduction of CD16 in a CD8 T cell clone was sufficient to increase HPV-VLP entry into these cells (data not shown).

NK cells play a key role in anti-viral and anti-tumoral responses by exocytosis of cytotoxic granules, and CD16 is a major receptor capable of triggering NK cytotoxicity (49). We showed that HPV-VLP induce the release of cytotoxic granules by NK and NK92 CD16+ cells, but not by NK92 CD16- cells (Fig. 8). In addition to killing infected cells, this degranulation process could liberate granulysin present in cytotoxic granules, which works as an alarmin and activates DC (64). Besides this degranulation activity, NK cells are able to

activate adaptive immune responses through the secretion of soluble factors such as IFN-γ and TNF-α (21, 22) and through cross-linking of CD16, which induces the secretion of these cytokines (65). NK and NK92 CD16+ cells but not NK92 CD16- secreted IFN-γ and TNF-α in response to HPV-VLP stimulation (Fig. 9). VLP were produced in insect cells infected with baculovirus coding for HPV16 L1. Because insect baculovirus contaminants have been reported to play a role in the immunogenicity induced by VLP (66), we used a lysate of insect cells infected with WT baculovirus as a negative control and we did not observe cytotoxic granule release or cytokine production in this culture condition. As described for DC activation (67), we showed that denaturation of VLP abolishes cytokine production by NK cells and exocytosis of cytotoxic granules. Activation of murine NK cells by VLP has already been reported for Ebola virus and activated NK cells have been shown to protect mice against Ebola infection (68).

Taken together, our results suggest that NK cells could participate in the high rate of spontaneous regression of HPV-associated preneoplastic lesions. Indeed, HPV infections are cleared in ~80% of women within 2 years (50). NK cells present in these preneoplastic lesions could be activated by L1 viral particles and kill HPV-infected cells. Alternatively, NK cells could help to induce an adaptive immune response against HPV by secreting cytokines. The presence of L1 seems to be important for dysplasia regression since this phenomenon has been correlated to L1 protein expression (69). Moreover, E7 protein from high-risk HPV has been shown to reduce cell surface expression of MHC Class I molecules (70), rendering these cells susceptible to lysis by NK cells. However, viruses have developed mechanisms to avoid immune response and some mechanisms are directed against NK cells. For example, direct infection of NK cells by vaccinia virus has been shown to negatively modulate NK cell function (71) and internalization of influenza virions in NK cells has also been described to cause a decrease in NK cytotoxicity (72). In patients with invasive cervical cancer, NK cells express a lower level of NKp30, NKp46 and NKG2D and have a lower capacity to kill tumor

cells compared to NK cells from healthy donors (73), suggesting that the immune escape mechanisms against NK cells occur in late-stage HPV-associated lesions. A better understanding of the role of NK cells in HPV-associated lesions could help to design a better vaccine and treatment strategy for this disease.

Acknowledgments

We thank Dr S. Ormenese from the GIGA-Imaging and Flow Cytometry platform for her support with flow cytometry and confocal microscopy. We are also grateful to Dr. P. Coursaget for the provision of baculovirus expressing HPV16 and HPV31 L1, Dr L. Bousarghin for providing electron microscopy grids with DC containing HPV-VLP, Prof. N. Christensen for providing V5 antibodies, M. Lebrun for her assistance with confocal microscopy and Prof. G. Thibault for helpful discussion..

References

1. zur Hausen, H. 2000. Papillomaviruses causing cancer: evasion from host-cell control in early events in carcinogenesis. *J Natl Cancer Inst* 92:690-698.
2. Daling, J. R., M. M. Madeleine, S. M. Schwartz, K. A. Shera, J. J. Carter, B. McKnight, P. L. Porter, D. A. Galloway, J. K. McDougall, and H. Tamimi. 2002. A population-based study of squamous cell vaginal cancer: HPV and cofactors. *Gynecol Oncol* 84:263-270.
3. zur Hausen, H. 1989. Papillomaviruses in anogenital cancer as a model to understand the role of viruses in human cancers. *Cancer Res* 49:4677-4681.
4. Chung, C. H., and M. L. Gillison. 2009. Human papillomavirus in head and neck cancer: its role in pathogenesis and clinical implications. *Clin Cancer Res* 15:6758-6762.
5. Castellsagué, X., S. de San Jose, T. Aguado, K. S. Louie, L. Bruni, J. Munoz, M. Diaz, K. Irwin, M. Gacic, O. Beauvais, G. Albero, E. Ferrer, S. Byrne, and F. X. Bosch. 2007. HPV and cervical cancer in the world, 2007 Report. *Vaccine* 25:C1-C230.
6. Dollard, S. C., J. L. Wilson, L. M. Demeter, W. Bonnez, R. C. Reichman, T. R. Broker, and L. T. Chow. 1992. Production of human papillomavirus and modulation of the infectious program in epithelial raft cultures. OFF. *Genes Dev* 6:1131-1142.
7. Le Cann, P., P. Coursaget, S. Iochmann, and A. Touze. 1994. Self-assembly of human papillomavirus type 16 capsids by expression of the L1 protein in insect cells. *FEMS Microbiol Lett* 117:269-274.
8. Da Silva, D. M., M. P. Velders, J. D. Nieland(4), J. T. Schiller, B. J. Nickoloff, and W. M. Kast. 2001. Physical interaction of human papillomavirus virus-like particles with immune cells. *Int Immunol* 13:633-641.

9. Lenz, P., P. M. Day, Y. Y. Pang, S. A. Frye, P. N. Jensen, D. R. Lowy, and J. T. Schiller. 2001. Papillomavirus-like particles induce acute activation of dendritic cells. *J Immunol* 166:5346-5355.
10. Olsson, S. E., L. L. Villa, R. L. Costa, C. A. Petta, R. P. Andrade, C. Malm, O. E. Iversen, J. Hoye, M. Steinwall, G. Riis-Johannessen, A. Andersson-Ellstrom, K. Elfgren, G. von Krogh, M. Lehtinen, J. Paavonen, G. M. Tamms, K. Giacoletti, L. Lupinacci, M. T. Esser, S. C. Vuocolo, A. J. Saah, and E. Barr. 2007. Induction of immune memory following administration of a prophylactic quadrivalent human papillomavirus (HPV) types 6/11/16/18 L1 virus-like particle (VLP) vaccine. *Vaccine* 25:4931-4939.
11. Paavonen, J., D. Jenkins, F. X. Bosch, P. Naud, J. Salmeron, C. M. Wheeler, S. N. Chow, D. L. Apter, H. C. Kitchener, X. Castellsague, N. S. de Carvalho, S. R. Skinner, D. M. Harper, J. A. Hedrick, U. Jaisamrarn, G. A. Limson, M. Dionne, W. Quint, B. Spiessens, P. Peeters, F. Struyf, S. L. Wieting, M. O. Lehtinen, and G. Dubin. 2007. Efficacy of a prophylactic adjuvanted bivalent L1 virus-like-particle vaccine against infection with human papillomavirus types 16 and 18 in young women: an interim analysis of a phase III double-blind, randomised controlled trial. *Lancet* 369:2161-2170.
12. Laniosz, V., S. A. Dabydeen, M. A. Havens, and P. I. Meneses. 2009. Human Papillomavirus Type 16 Infection of Human Keratinocytes Requires Clathrin, Caveolin-1, and is Brefeldin A-sensitive. *J Virol* 83:8221-8232.
13. Broutian, T. R., S. A. Brendle, and N. D. Christensen. 2010. Differential binding patterns to host cells associated with particles of several human alphapapillomavirus types. *J Gen Virol* 91:531-540.
14. Muller, M., L. Gissmann, R. J. Cristiano, X. Y. Sun, I. H. Frazer, A. B. Jenson, A. Alonso, H. Zentgraf, and J. Zhou. 1995. Papillomavirus capsid binding and uptake by cells from different tissues and species. *J Virol* 69:948-954.
15. Bousarghin, L., P. Hubert, E. Franzen, N. Jacobs, J. Boniver, and P. Delvenne. 2005. Human papillomavirus 16 virus-like particles use heparan sulfates to bind dendritic cells and colocalize with langerin in Langerhans cells. *J Gen Virol* 86:1297-1305.
16. de Witte, L., Y. Zoughlami, B. Aengeneyndt, G. David, Y. van Kooyka, L. Gissmannb, and T. B. H. Geijtenbeeka. 2008. Binding of human papilloma virus L1 virus-like particles to dendritic cells is mediated through heparan sulfates and induces immune activation *Immunobiology* 212:679-691.
17. Biron, C. A. 2010. Expansion, maintenance, and memory in NK and T cells during viral infections: responding to pressures for defense and regulation. *PLoS Pathog* 6:e1000816.
18. Biron, C. A., K. S. Byron, and J. L. Sullivan. 1989. Severe herpesvirus infections in an adolescent without natural killer cells. *N Engl J Med* 320:1731-1735.
19. Waldhauer, I., and A. Steinle. 2008. NK cells and cancer immunosurveillance. *Oncogene* 27:5932-5943.
20. Walzer, T., M. Blery, J. Chaix, N. Fuseri, L. Chasson, S. H. Robbins, S. Jaeger, P. Andre, L. Gauthier, L. Daniel, K. Chemin, Y. Morel, M. Dalod, J. Imbert, M. Pierres, A. Moretta, F. Romagne, and E. Vivier. 2007. Identification, activation, and selective in vivo ablation of mouse NK cells via NKp46. *Proceedings of the National Academy of Sciences of the United States of America* 104:3384-3389.
21. Vivier, E., E. Tomasello, M. Baratin, T. Walzer, and S. Ugolini. 2008. Functions of natural killer cells. *Nat Immunol* 9:503-510.
22. Caligiuri, M. A. 2008. Human natural killer cells. *Blood* 112:461-469.
23. Chavez-Galan, L., M. C. Arenas-Del Angel, E. Zenteno, R. Chavez, and R. Lascurain. 2009. Cell death mechanisms induced by cytotoxic lymphocytes. *Cell Mol Immunol* 6:15-25.

24. Herberman, R. B., C. W. Reynolds, and J. R. Ortaldo. 1986. Mechanism of cytotoxicity by natural killer (NK) cells. *Annu Rev Immunol* 4:651-680.
25. Perussia B, T. G., Jackson A, Warner NL, Faust J, Rumpold H, Kraft D and Lanier LL 1984. The Fc receptor for IgG on human natural killer cells: phenotypic, functional, and comparative studies with monoclonal antibodies. *J Immunol* 133:180-189.
26. Lanier, L. L., J. H. Phillips, J. Hackett, Jr., M. Tutt, and V. Kumar. 1986. Natural killer cells: definition of a cell type rather than a function. *J Immunol* 137:2735-2739.
27. Da Silva, D., S. Fausch, J. Verbeek, and W. Kast. 2007. Uptake of Human Papillomavirus Virus-Like Particles by Dendritic Cells Is Mediated by Fc{gamma} Receptors and Contributes to Acquisition of T Cell Immunity. *J Immunol* 178:7587-7597.
28. Guidotti, L. G., and F. V. Chisari. 2001. Noncytolytic control of viral infections by the innate and adaptive immune response. *Annu Rev Immunol* 19:65-91.
29. Fehniger, T. A., M. A. Cooper, G. J. Nuovo, M. Cella, F. Facchetti, M. Colonna, and M. A. Caligiuri. 2003. CD56bright natural killer cells are present in human lymph nodes and are activated by T cell-derived IL-2: a potential new link between adaptive and innate immunity. *Blood* 101:3052-3057.
30. King, A., T. Burrows, and Y. W. Loke. 1996. Human uterine natural killer cells. *Nat Immun* 15:41-52.
31. Fuller, C. L., G. Ruthel, K. L. Warfield, D. L. Swenson, C. M. Bosio, M. J. Aman, and S. Bavari. 2007. NKp30-dependent cytolysis of filovirus-infected human dendritic cells. *Cell Microbiol* 9:962-976.
32. Kobayashi, A., R. M. Greenblatt, K. Anastos, H. Minkoff, L. S. Massad, M. Young, A. M. Levine, T. M. Darragh, V. Weinberg, and K. K. Smith-McCune. 2004. Functional attributes of mucosal immunity in cervical intraepithelial neoplasia and effects of HIV infection. *Cancer Res* 64:6766-6774.
33. Gong, J. H., G. Maki, and H. G. Klingemann. 1994. Characterization of a human cell line (NK-92) with phenotypical and functional characteristics of activated natural killer cells. *Leukemia* 8:652-658.
34. Clemenceau, B., N. Congy-Jolivet, G. Gallot, R. Vivien, J. Gaschet, G. Thibault, and H. Vie. 2006. Antibody-dependent cellular cytotoxicity (ADCC) is mediated by genetically modified antigen-specific human T lymphocytes. *Blood* 107:4669-4677.
35. Touze, A., C. Dupuy, D. Mahe, P. Y. Sizaret, and P. Coursaget. 1998. Production of recombinant virus-like particles from human papillomavirus types 6 and 11, and study of serological reactivities between HPV 6, 11, 16 and 45 by ELISA: implications for papillomavirus prevention and detection. *FEMS Microbiol Lett* 160:111-118.
36. Christensen, N. D., J. Dillner, C. Eklund, J. J. Carter, G. C. Wipf, C. A. Reed, N. M. Cladel, and D. A. Galloway. 1996. Surface conformational and linear epitopes on HPV-16 and HPV-18 L1 virus-like particles as defined by monoclonal antibodies. *Virology* 223:174-184.
37. Bergsdorf, C., C. Beyer, V. Umansky, M. Werr, and M. Sapp. 2003. Highly efficient transport of carboxyfluorescein diacetate succinimidyl ester into COS7 cells using human papillomavirus-like particles. *FEBS Lett* 536:120-124.
38. Ho, T. T., S. D. Merajver, C. M. Lapiere, B. V. Nusgens, and C. F. Deroanne. 2008. RhoA-GDP regulates RhoB protein stability. Potential involvement of RhoGDIalpha. *J Biol Chem* 283:21588-21598.
39. Burghardt, E., and A. G. Ostor. 1983. Site and origin of squamous cervical cancer: a histomorphologic study. *Obstet Gynecol* 62:117-127.
40. Arafa, M., J. Boniver, and P. Delvenne. 2008. Detection of HPV-induced cervical (pre) neoplastic lesions: a tissue microarray (TMA) study. *Appl Immunohistochem Mol Morphol* 16:422-432.

41. Yoshida, T., T. Sano, T. Kanuma, N. Owada, S. Sakurai, T. Fukuda, and T. Nakajima. 2008. Immunochemical analysis of HPV L1 capsid protein and p16 protein in liquid-based cytology samples from uterine cervical lesions. *Cancer* 114:83-88.
42. Hopman, A. H., F. Smedts, W. Dignef, M. Ummelen, G. Sonke, M. Mravunac, G. P. Vooijs, E. J. Speel, and F. C. Ramaekers. 2004. Transition of high-grade cervical intraepithelial neoplasia to micro-invasive carcinoma is characterized by integration of HPV 16/18 and numerical chromosome abnormalities. *J Pathol* 202:23-33.
43. Mercer, J., and A. Helenius. 2009. Virus entry by macropinocytosis. *Nat Cell Biol* 11:510-520.
44. Sieczkarski, S. B., and G. R. Whittaker. 2002. Dissecting virus entry via endocytosis. *Journal of General Virology* 83:1535-1545.
45. Bousarghin, L., A. Touze, P. Y. Sizaret, and P. Coursaget. 2003. Human papillomavirus types 16, 31, and 58 use different endocytosis pathways to enter cells. *J Virol* 77:3846-3850.
46. Laniosz, V., S. A. Dabydeen, M. A. Havens, and P. I. Meneses. 2009. Human papillomavirus type 16 infection of human keratinocytes requires clathrin and caveolin-1 and is brefeldin a sensitive. *J Virol* 83:8221-8232.
47. Joyce, J. G., J. S. Tung, C. T. Przysiecki, J. C. Cook, E. D. Lehman, J. A. Sands, K. U. Jansen, and P. M. Keller. 1999. The L1 major capsid protein of human papillomavirus type 11 recombinant virus-like particles interacts with heparin and cell-surface glycosaminoglycans on human keratinocytes. *J Biol Chem* 274:5810-5822.
48. Rubio, V., T. B. Stuge, N. Singh, M. R. Betts, J. S. Weber, M. Roederer, and P. P. Lee. 2003. Ex vivo identification, isolation and analysis of tumor-cytolytic T cells. *Nat Med* 9:1377-1382.
49. Bryceson, Y. T., M. E. March, D. F. Barber, H. G. Ljunggren, and E. O. Long. 2005. Cytolytic granule polarization and degranulation controlled by different receptors in resting NK cells. *J Exp Med* 202:1001-1012.
50. Rodriguez, A. C., M. Schiffman, R. Herrero, S. Wacholder, A. Hildesheim, P. E. Castle, D. Solomon, and R. Burk. 2008. Rapid clearance of human papillomavirus and implications for clinical focus on persistent infections. *J Natl Cancer Inst* 100:513-517.
51. Didierlaurent, A. M., S. Morel, L. Lockman, S. L. Giannini, M. Bisteau, H. Carlsen, A. Kielland, O. Vosters, N. Vanderheyde, F. Schiavetti, D. Larocque, M. Van Mechelen, and N. Garcon. 2009. AS04, an aluminum salt- and TLR4 agonist-based adjuvant system, induces a transient localized innate immune response leading to enhanced adaptive immunity. *J Immunol* 183:6186-6197.
52. Parolini, S., A. Santoro, E. Marcenaro, W. Luini, L. Massardi, F. Facchetti, D. Communi, M. Parmentier, A. Majorana, M. Sironi, G. Tabellini, A. Moretta, and S. Sozzani. 2007. The role of chemerin in the colocalization of NK and dendritic cell subsets into inflamed tissues. *Blood* 109:3625-3632.
53. Sandel, M. H., F. M. Speetjens, A. G. Menon, P. A. Albertsson, P. H. Basse, M. Hokland, J. F. Nagelkerke, R. A. Tollenaar, C. J. van de Velde, and P. J. Kuppen. 2005. Natural killer cells infiltrating colorectal cancer and MHC class I expression. *Mol Immunol* 42:541-546.
54. Smith, J. L., S. K. Campos, and M. A. Ozbun. 2007. Human papillomavirus type 31 uses a caveolin 1- and dynamin 2-mediated entry pathway for infection of human keratinocytes. *J Virol*.
55. Drobni, P., N. Mistry, N. McMillan, and E. Magnus. 2003. Carboxy-fluorescein diacetate, succinimidyl ester labeled papillomavirus virus-like particles fluorece after internalization and interact with heparan sulfate for binding and entry. *Virology* 310:163-172.

56. Horvath, C. A., G. A. Boulet, V. M. Renoux, P. O. Delvenne, and J. P. Bogers. 2010. Mechanisms of cell entry by human papillomaviruses: an overview. *Virol J* 7:11.
57. Ladwein, M., and K. Rottner. 2008. On the Rho'd: the regulation of membrane protrusions by Rho-GTPases. *FEBS Lett* 582:2066-2074.
58. Nobes, C. D., and A. Hall. 1995. Rho, rac, and cdc42 GTPases regulate the assembly of multimolecular focal complexes associated with actin stress fibers, lamellipodia, and filopodia. *Cell* 81:53-62.
59. Zamudio-Meza, H., A. Castillo-Alvarez, C. Gonzalez-Bonilla, and I. Meza. 2009. Cross-talk between Rac1 and Cdc42 GTPases regulates formation of filopodia required for dengue virus type-2 entry into HMEC-1 cells. *J Gen Virol* 90:2902-2911.
60. Mercer, J., S. Knebel, F. I. Schmidt, J. Crouse, C. Burkard, and A. Helenius. 2010. Vaccinia virus strains use distinct forms of macropinocytosis for host-cell entry. *Proceedings of the National Academy of Sciences of the United States of America* 107:9346-9351.
61. Araki, N., T. Hatae, A. Furukawa, and J. A. Swanson. 2003. Phosphoinositide-3-kinase-independent contractile activities associated with Fcgamma-receptor-mediated phagocytosis and macropinocytosis in macrophages. *J Cell Sci* 116:247-257.
62. Wu, Y., W. Wu, W. M. Wong, E. Ward, A. J. Thrasher, D. Goldblatt, M. Osman, P. Digard, D. H. Canaday, and K. Gustafsson. 2009. Human γδ T cells : a lymphoid lineage cell capable of professional phagocytosis. *J. Immunol* 183:5622-5629.
63. Jarahian, M., C. Watzl, P. Fournier, A. Arnold, D. Djandji, S. Zahedi, A. Cerwenka, A. Paschen, V. Schirrmacher, and F. Momburg. 2009. Activation of natural killer cells by newcastle disease virus hemagglutinin-neuraminidase. *J Virol* 83:8108-8121.
64. Tewary, P., D. Yang, G. de la Rosa, Y. Li, M. W. Finn, A. M. Krensky, C. Clayberger, and J. J. Oppenheim. 2010. Granulysin activates antigen-presenting cells through TLR4 and acts as an immune alarmin. *Blood* 116:3465-3474.
65. Marquez, M. E., C. Millet, H. Stekman, A. Conesa, P. A. Deglesne, F. Toro, J. D. Sanctis, and I. Blanca. 2010. CD16 cross-linking induces increased expression of CD56 and production of IL-12 in peripheral NK cells. *Cell Immunol* 264:86-92.
66. Hervas-Stubbs, S., P. Rueda, L. Lopez, and C. Leclerc. 2007. Insect baculoviruses strongly potentiate adaptive immune responses by inducing type I IFN. *J Immunol* 178:2361-2369.
67. Rudolf, M. P., S. C. Fausch, D. M. Da Silva, and W. M. Kast. 2001. Human dendritic cells are activated by chimeric human papillomavirus type-16 virus-like particles and induce epitope-specific human T cell responses in vitro. *J Immunol* 166:5917-5924.
68. Warfield, K. L., J. G. Perkins, D. L. Swenson, E. M. Deal, C. M. Bosio, M. J. Aman, W. M. Yokoyama, H. A. Young, and S. Bavari. 2004. Role of natural killer cells in innate protection against lethal ebola virus infection. *J Exp Med* 200:169-179.
69. Griesser, H., H. Sander, R. Hilfrich, B. Moser, and U. Schenck. 2004. Correlation of immunochemical detection of HPV L1 capsid protein in pap smears with regression of high-risk HPV positive mild/moderate dysplasia. *Anal Quant Cytol Histol* 26:241-245.
70. Bottley, G., O. G. Watherston, Y. L. Hiew, B. Norrild, G. P. Cook, and G. E. Blair. 2008. High-risk human papillomavirus E7 expression reduces cell-surface MHC class I molecules and increases susceptibility to natural killer cells. *Oncogene* 27:1794-1799.
71. Kirwan, S., D. Merriam, N. Barsby, A. McKinnon, and D. N. Burshtyn. 2006. Vaccinia virus modulation of natural killer cell function by direct infection. *Virology* 347:75-87.
72. Mao, H., W. Tu, Y. Liu, G. Qin, J. Zheng, P. L. Chan, K. T. Lam, J. S. Peiris, and Y. L. Lau. 2010. Inhibition of human natural killer cell activity by influenza virions and hemagglutinin. *J Virol* 84:4148-4157.

73. Garcia-Iglesias, T., A. Del Toro-Arreola, B. Albarran-Somoza, S. Del Toro-Arreola, P. E. Sanchez-Hernandez, M. G. Ramirez-Duenas, L. M. Balderas-Pena, A. Bravo-Cuellar, P. C. Ortiz-Lazareno, and A. Daneri-Navarro. 2009. Low NKp30, NKp46 and NKG2D expression and reduced cytotoxic activity on NK cells in cervical cancer and precursor lesions. *BMC Cancer* 9:186.

Figure legends

Figure 1:

NKp46+ cells in cervical tissue samples. (A) Normal endocervical and (B) exocervical mucosa showing NKp46+ cells located in the subepithelial stroma. (C) Squamous intraepithelial lesion (SIL) with NKp46+ cells in the dysplastic epithelium, in addition to the stromal infiltrate. Inset: close-up view of a positive intraepithelial cell. (D) Invasive SCC demonstrating only few NKp46+ cells in the tumor, but increased numbers in the peritumoral stroma. (E) NKp46+ cell quantifications in the stroma, showing significantly more positive cells in the peritumoral stroma of SCC (n=14) compared to SIL (n=23), exocervix (n=19) or endocervix (n=8). (F) NKp46+ cell countings in the epithelium, demonstrating significantly more positive cells infiltrating the epithelium of SIL compared to exocervix and endocervix; countings in SCC were not statistically different from the other categories. Original magnification: A-D, x200; C inset: x1000. (Ep: epithelium; St: stroma; Endo: endocervix; Exo: exocervix; SIL: squamous intraepithelial lesion; SCC: squamous cell carcinoma; NS: not significant; *$p<0.05$; ** $p<0.01$)

Figure 2:

Uptake of HPV-VLP by NK cells. (A) Kinetics of HPV16-VLP-CFDA-SE internalization by blood NK cells (plain line) and CasKi cell line (dotted line) at 37 °C (mean ± SE, $n \geq 4$). (B) Fluorescence of HPV16-VLP-CFDA-SE internalization in DC produced *in vitro* (dotted line) and sorted NK cells (plain line) from the same donor after 10 min of incubation with HPV16 VLP-CFDA-SE (representative experiment of 4). (C) Similar HPV16 and HPV31 VLP-CFDA-SE internalization by NK cells after 10 min or 3 h (mean ± SE, $n \geq 6$). (D) Significant lower internalization of HPV16 VLP-CFDA-SE in NK cells at 4 °C or with HPV16 VLP-CFDA-SE heated for 10 min at 95 °C (6 h of incubation, mean ± SE, n =6) ** = $p<0.005$; *** = $p<0.001$.

Figure 3:

Confocal microscopy of HPV16 VLP-CFDA-SE internalization. (A) NK cells after 10 min in the presence of HPV-VLP, (B) DC and (C) CasKi cells both after 5h in the presence of HPV-VLP, no fluorescence was detected after 10 min in these cells. Objective: UPLSAPO 60X / NA 1.35.

Figure 4:

Electron microscopy of HPV16-VLP internalization. (A) Large vacuole containing VLP in NK cells after 10 min or (B) 6 h in the presence of HPV16-VLP, (C) small clathrin-coated vacuole containing one VLP (arrow) in DC incubated for 1 h in the presence of HPV16-VLP. (D-E) Membrane ruffles of NK cells surrounding VLP (arrows) after 10 min of incubation in the presence of HPV16-VLP.

Figure 5:

Entry of HPV16-VLP into NK cells is mediated by macropinocytosis. (A) HPV16-VLP (black squares) induce FITC-Dextran uptake in NK cells but not a lysate of insect cells infected with WT baculovirus (black triangles) or VLP disrupted by heating (black circles), in the presence of cytochalasin D (white squares) the uptake of extracellular fluid was inhibited (means ± SE of fluorescence fold increase over the control condition, n = 3, ** $p<0.005$). (B) GTPase assays on NK cells showed an activation of Cdc42 and a decreased activity of Rac1 in the presence HPV16-VLP. Cell lysates probed for total Cdc42 and Rac1 are shown as the loading control (bottom). These results represent 1 of 3 independent experiments. (C) Drugs inhibiting the clathrin (chlorpromazine) or caveola (nystatin) pathway did not affect significantly HPV16-VLP entry into NK cells after 10 min or 3 h of incubation. The percentages shown are related to HPV16-VLP internalization without inhibitors (means ± SE, n = 6-9).

Figure 6:

Entry of HPV-VLP into NK cells is dependent on CD16 expression. (A-B) Entry of CFDA-SE HPV16-VLP increased with higher level of CD16: NK92 CD16- (no CD16 expression) < NK92 CD16+/- (NK92 cells transduced with CD16, ratio of mean CD6 fluorescence = 10) < NK92 CD16+ sorted (NK92 cells transduced with CD16 and sorted by flow cytometry for their high CD16 cell surface expression, ratio of mean CD16 fluorescence = 28) < NK cells (NK cells sorted from blood, ratio of mean CD16 fluorescence = 98). Similar results were obtained after 10 min (A) or 3 h (B) of incubation in the presence of HPV16-VLP (means ± SE, n ≤ 3). (C-D) Confocal microscopy of CFDA-SE HPV16-VLP entry after 10 min of incubation into the NK92 cell line transduced with CD16 and CD16++ sorted (C) or into the NK92 CD16- cell line (D). (E-F) FITC-dextran assays: HPV16-VLP (black squares) induced FITC-Dextran uptake only in NK92 CD16+ cells (E) but not a lysate of insect cells infected with WT baculovirus (black triangles) or VLP disrupted by heating (black circles), in the presence of cytochalasin D (white squares) extracellular fluid uptake was inhibited. No significant fluid uptake was observed in NK92 CD16- cells (F) for any of the conditions tested (means ± SE of fluorescence fold increase over the control condition, n = 4), (* $p<0.05$, ** $p<0.005$, *** $p<0.001$).

Figure 7:

Down-modulation of CD16 in the presence of HPV16-VLP. Relative mean fluorescence of CD16 on the surface of NK cells (A) and NK92CD16+ (B) cells or relative mean fluorescence of NKp46 on the surface of NK cells (C) in the presence of HPV16-VLP are shown (mean fluorescence in the absence of VLP = 1, means ± SE, n=4,*$p<0.05$, **$p<0.005$, ***$p<0.0005$).

Figure 8:

HPV-VLP induce cytotoxic granule exocytosis in NK cells. Ratio of degranulation in NK cells (A), NK92 CD16+ (B) and NK92 CD16- (C) in the presence of HPV16-VLP, anti-CD16

mAb, a lysate of insect cells infected with WT baculovirus (WT) or PMA/ionophore after 1 h (A-C) or 6 h (A) of incubation. The percentage of CD107a+ cells of all conditions are divided by the percentage of CD107a+ cells in the control condition (medium alone) (means ± SE, n>3, *p<0.05).

Figure 9:

HPV-VLP induce cytokine secretion in NK cells. TNF-α (A) and IFN-γ (B) ELISA assays on 24 h culture supernatant of NK and NK92 CD16+ cells incubated in the presence of HPV16-VLP, CD16 mAb, or a lysate of insect cells infected with WT baculovirus (WT) (means ± SE, n>3).

Supplementary files

Supplementary files S1:

Uptake of HPV16-VLP by NK cells. HPV-16-VLP-CFDA-SE internalization by NK cells is dose dependant (Fig. S1A). Significant lower internalization of HPV16-VLP-CFDA-SE in NK cells after a saturation of receptors with unlabelled HPV-VLP (Fig. S1B).

Supplementary files S2:

Uptake of HPV16-VLP by NK cells, after 10 minutes or 3 hours of incubation, is significantly reduced by an incubation of NK cells with heparinase II.

Supplementary files S3:

Kinetics of HPV16-VLP-CFDA-SE internalization by NK92 cell line (CD16-, dotted line) and CasKi cell line (plain line) at 37°C (mean ± SE, n = 4).

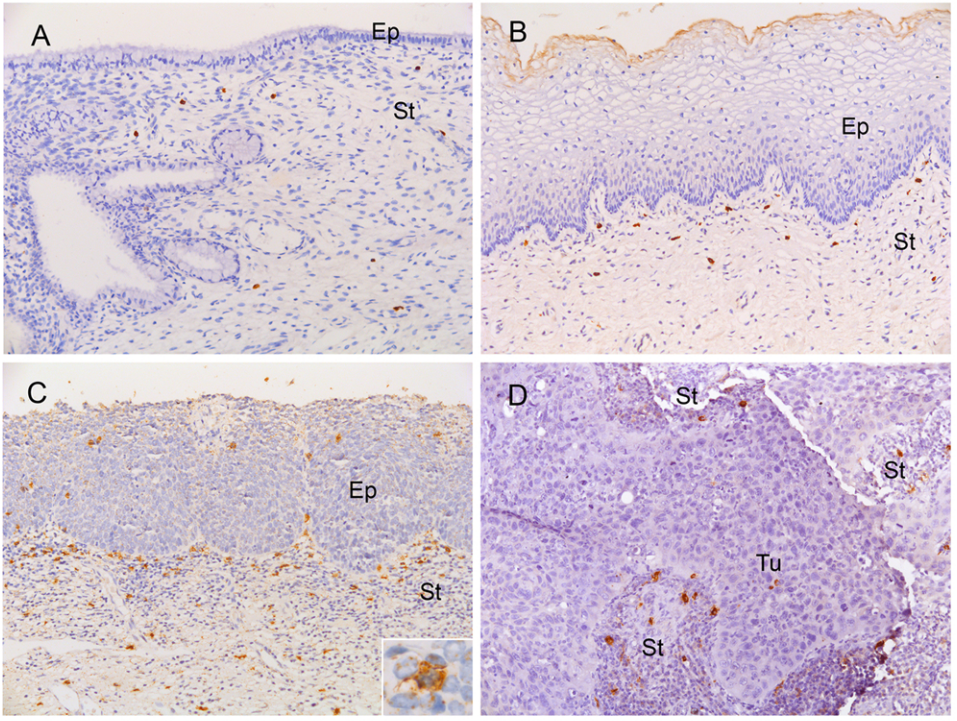
A
Ep
St
B
Ep
St
C
Ep
St
D
St
St
Tu
St

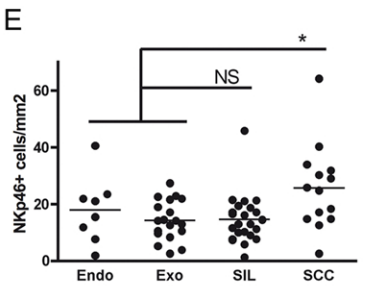
E
NKp46+ cells/mm2
0
20
40
60
*
NS
Endo
Exo
SIL
SCC

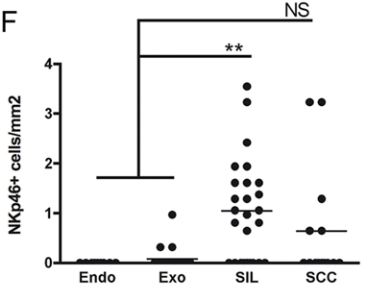
F
NKp46+ cells/mm2
0
1
2
3
4
NS
**
Endo
Exo
SIL
SCC

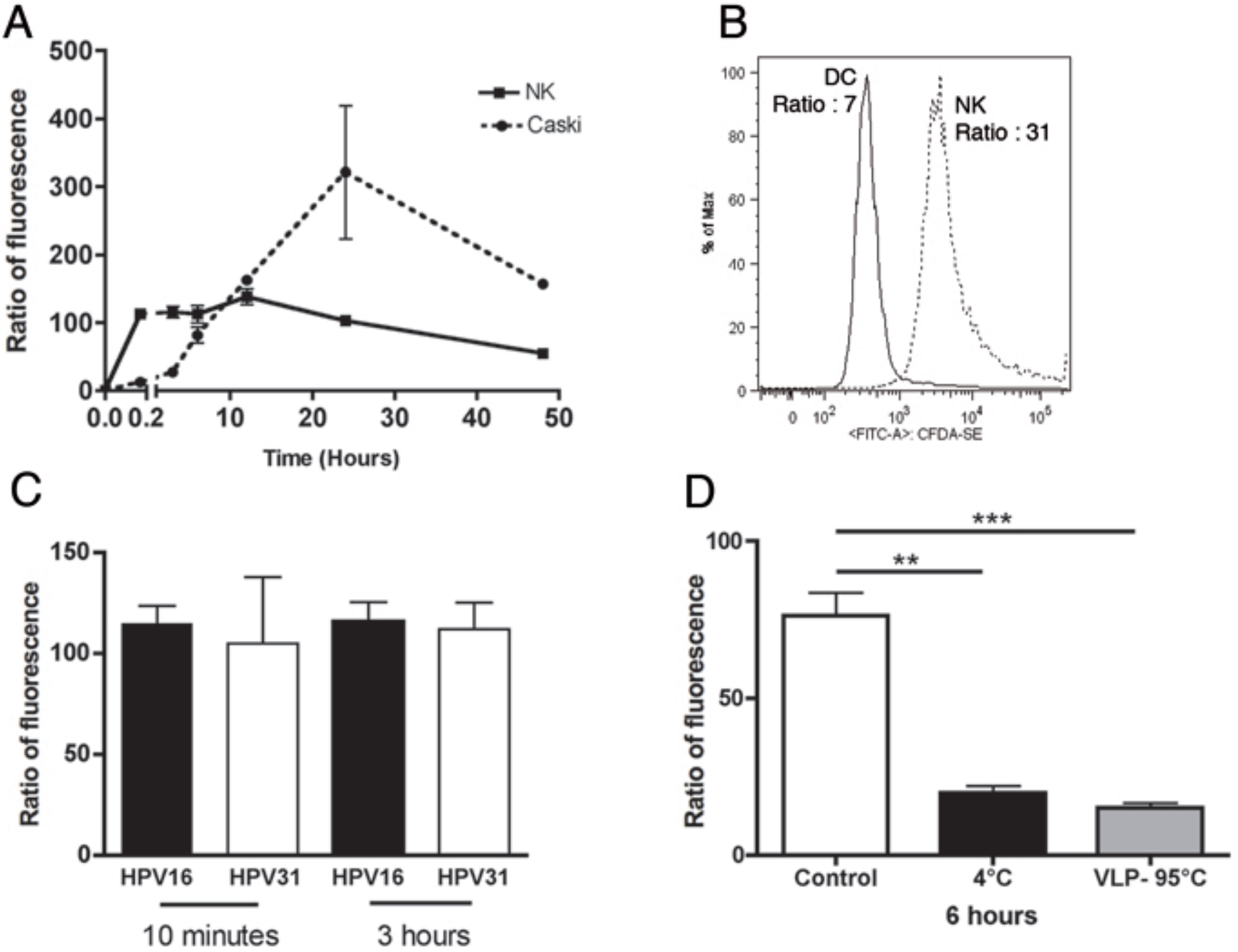
A
Ratio of fluorescence
500
400
300
200
100
0
NK
Caski
0.0 0.2
10
20
30
40
50
Time (Hours)
B
DC
Ratio : 7
NK
Ratio : 31
% of Max
100
80
60
40
20
0
0
10^2
10^3
10^4
10^5
<FITC-A>: CFDA-SE
C
Ratio of fluorescence
150
100
50
0
HPV16
HPV31
HPV16
HPV31
10 minutes
3 hours
D
***
**
Ratio of fluorescence
100
50
0
Control
4°C
VLP- 95°C
6 hours

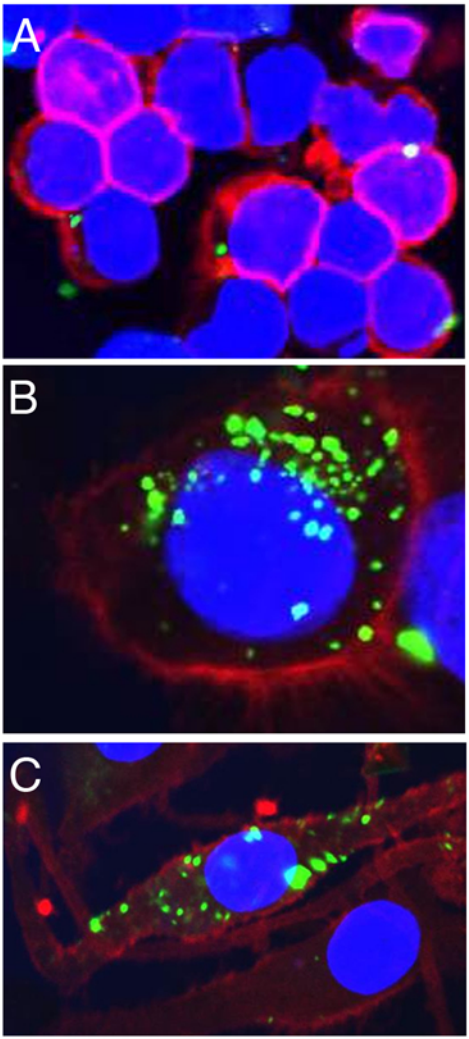
A
B
C

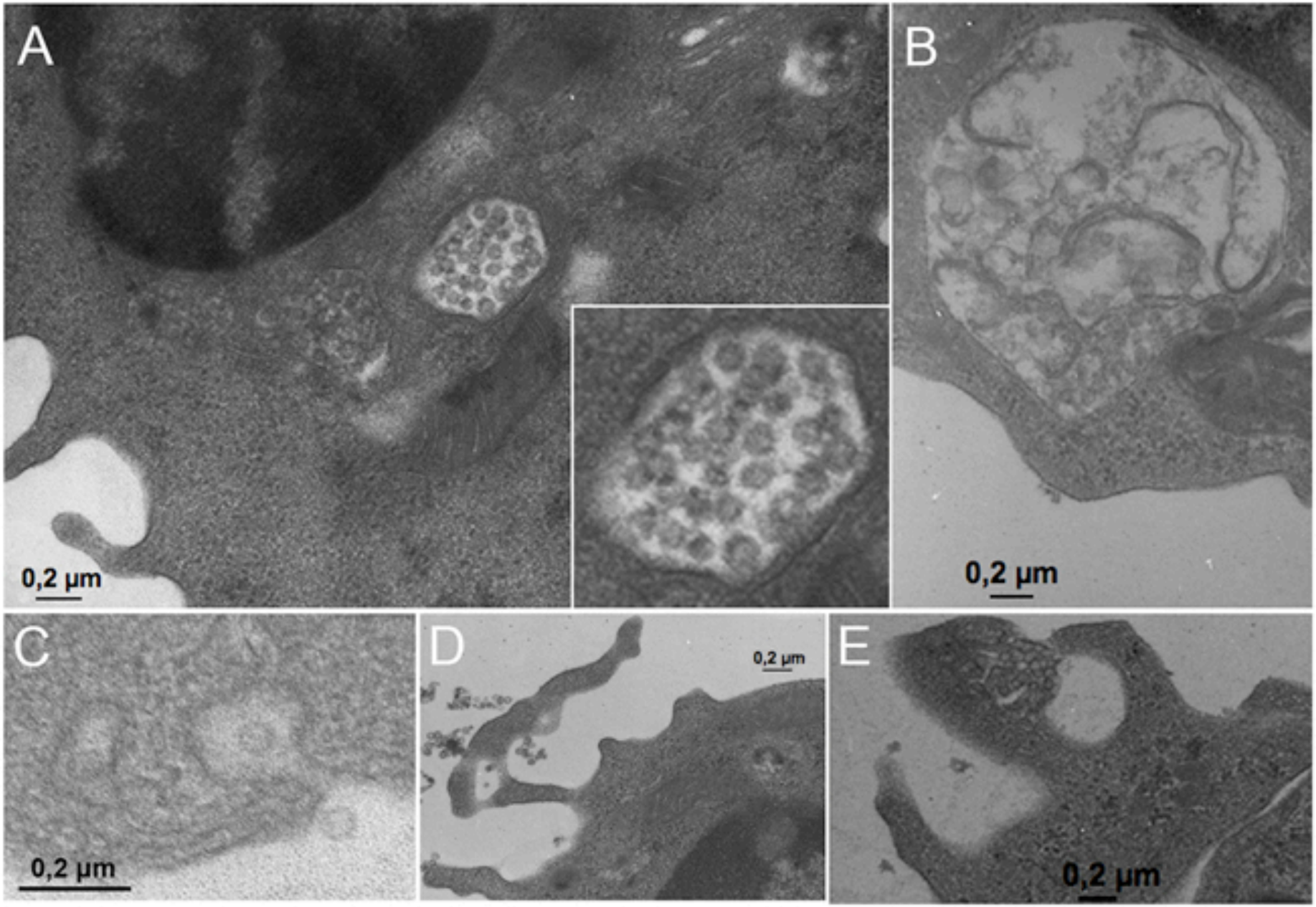
A
0,2 µm
B
0,2 µm
C
0,2 µm
D
0,2 µm
E
0,2 µm

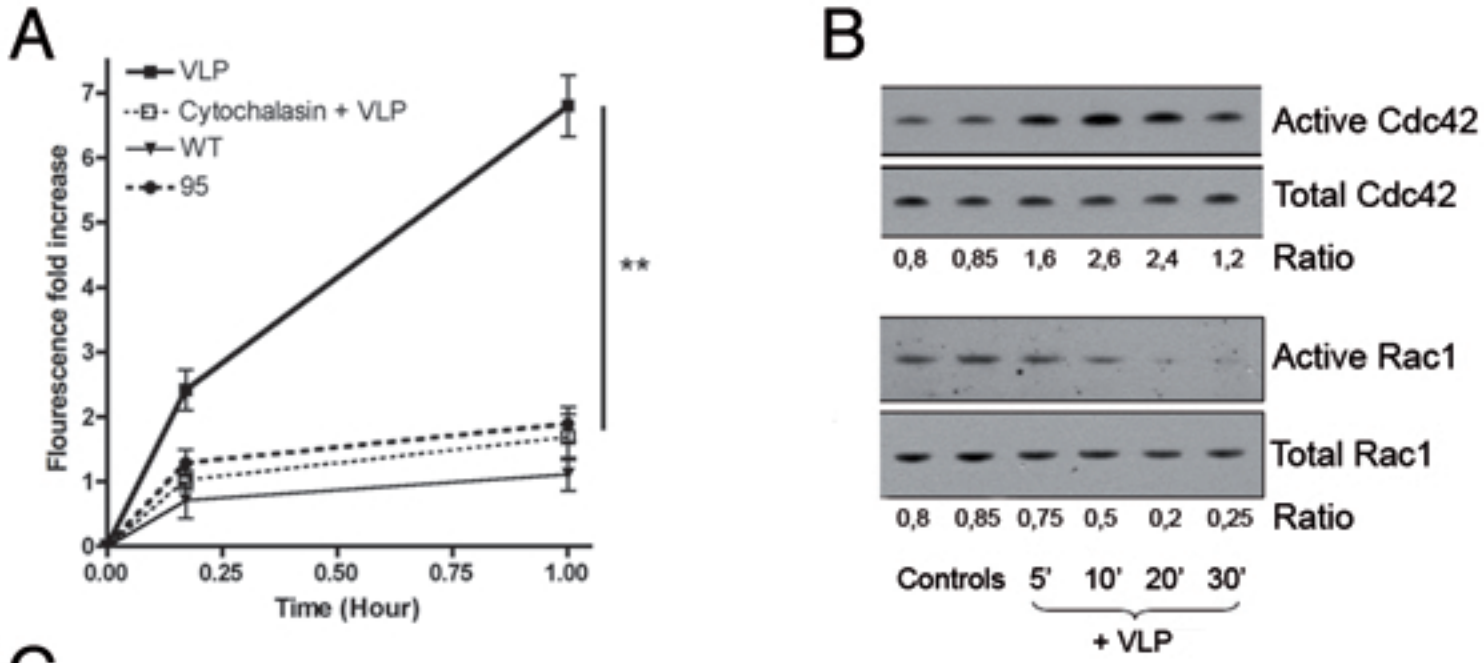
A
VLP
Cytochalasin + VLP
WT
95
Flourescence fold increase
Time (Hour)
**
B
Active Cdc42
Total Cdc42
0,8 0,85 1,6 2,6 2,4 1,2
Ratio
Active Rac1
Total Rac1
0,8 0,85 0,75 0,5 0,2 0,25
Ratio
Controls 5' 10' 20' 30'
+ VLP

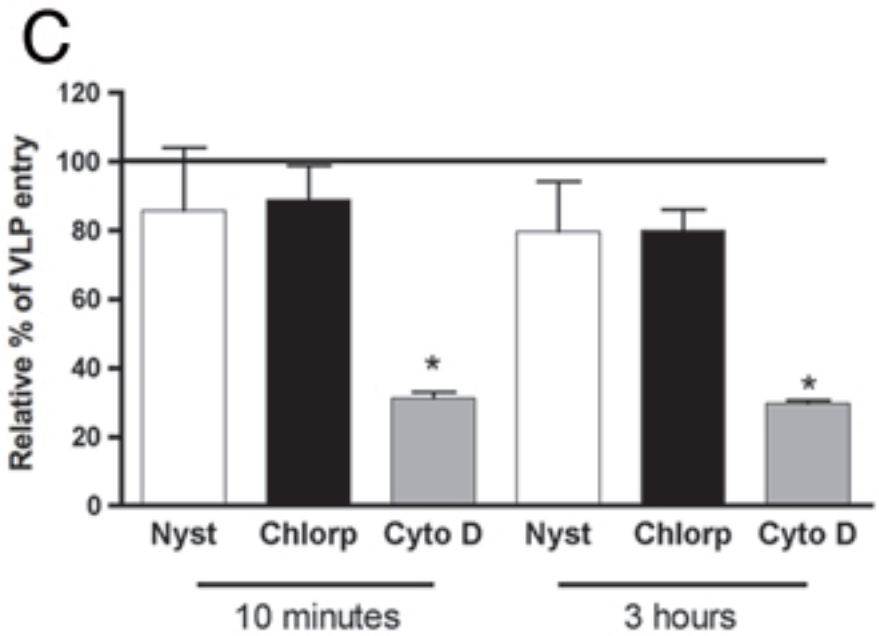
C
Relative % of VLP entry
Nyst Chlorp Cyto D Nyst Chlorp Cyto D
10 minutes
3 hours

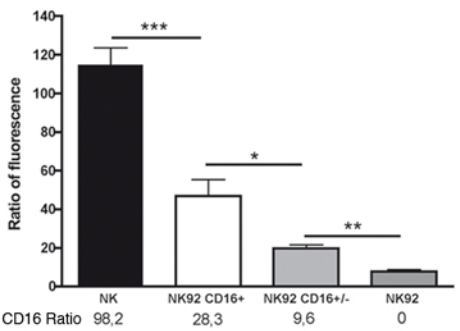
A
Ratio of fluorescence
140
120
100
80
60
40
20
0
***
*
**
NK
NK92 CD16+
NK92 CD16+/-
NK92
CD16 Ratio 98,2
28,3
9,6
0

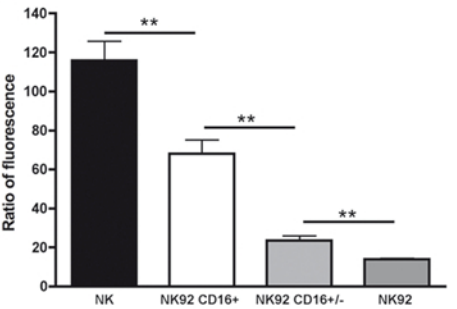
B
Ratio of fluorescence
140
120
100
80
60
40
20
0
**
**
**
NK
NK92 CD16+
NK92 CD16+/-
NK92

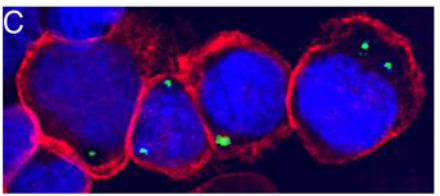
C

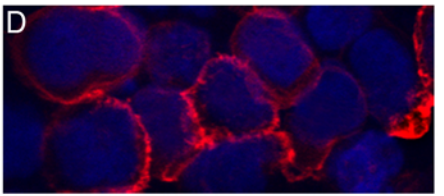
D

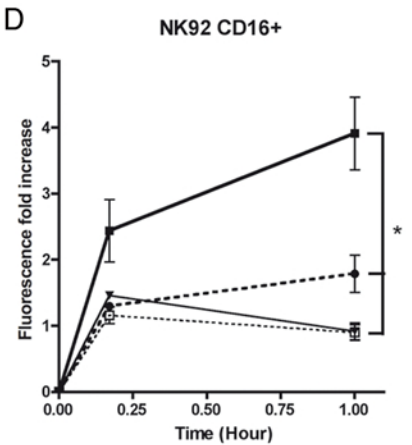
D
NK92 CD16+
Fluorescence fold increase
5
4
3
2
1
0
*
0.00
0.25
0.50
0.75
1.00
Time (Hour)

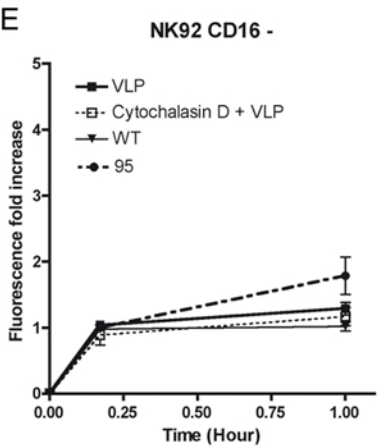
E
NK92 CD16 -
VLP
Cytochalasin D + VLP
WT
95
Fluorescence fold increase
5
4
3
2
1
0
0.00
0.25
0.50
0.75
1.00
Time (Hour)

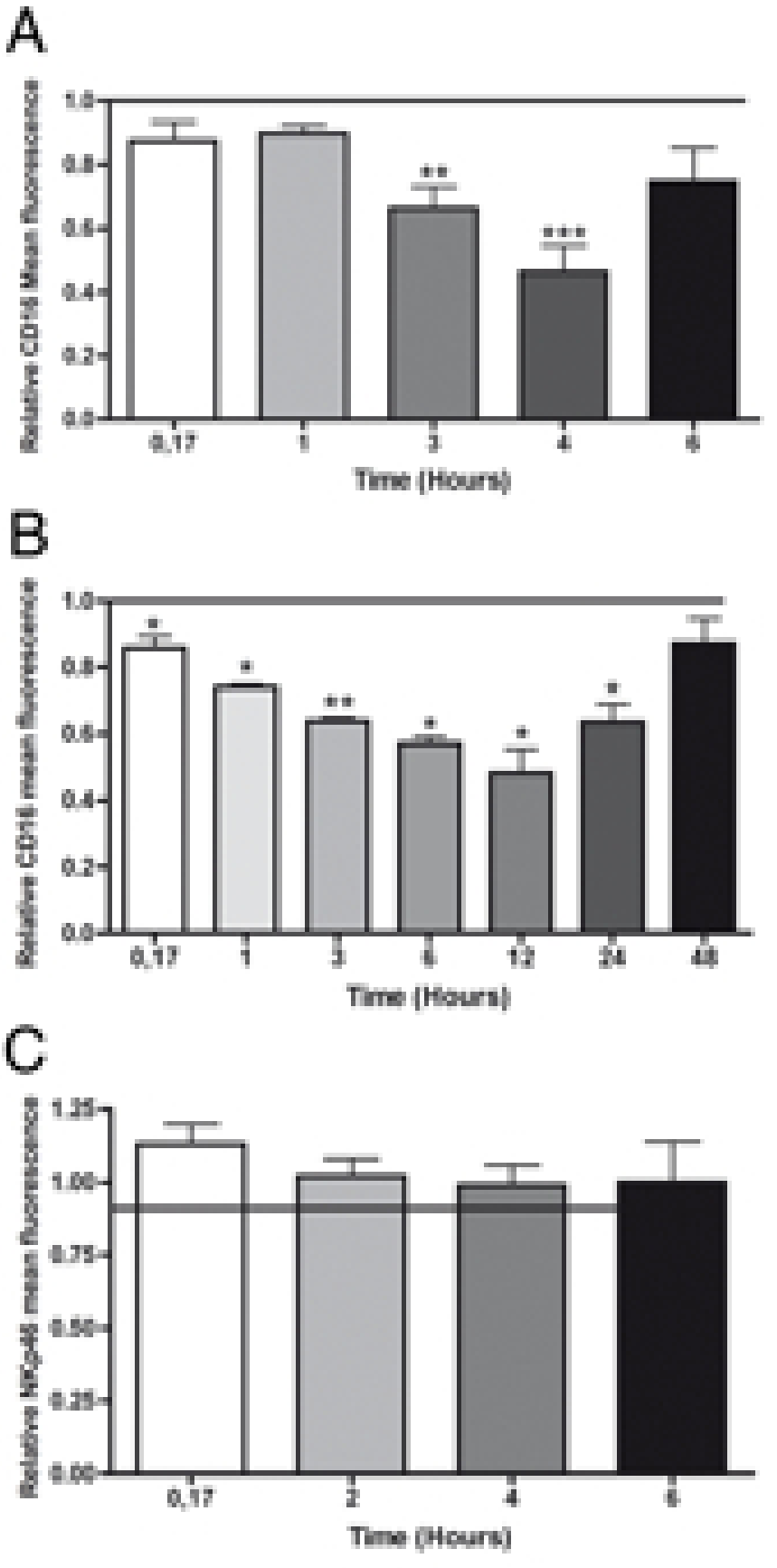
A
Relative CD16 Mean fluorescence
1.0
0.8
0.6
0.4
0.2
0.0
**
***
0,17
1
3
4
6
Time (Hours)
B
Relative CD16 mean fluorescence
1.0
0.8
0.6
0.4
0.2
0.0
*
*
**
*
*
*
*
0,17
1
3
6
12
24
48
Time (Hours)
C
Relative NKp46 mean fluorescence
1.25
1.00
0.75
0.50
0.25
0.00
0,17
2
4
6
Time (Hours)

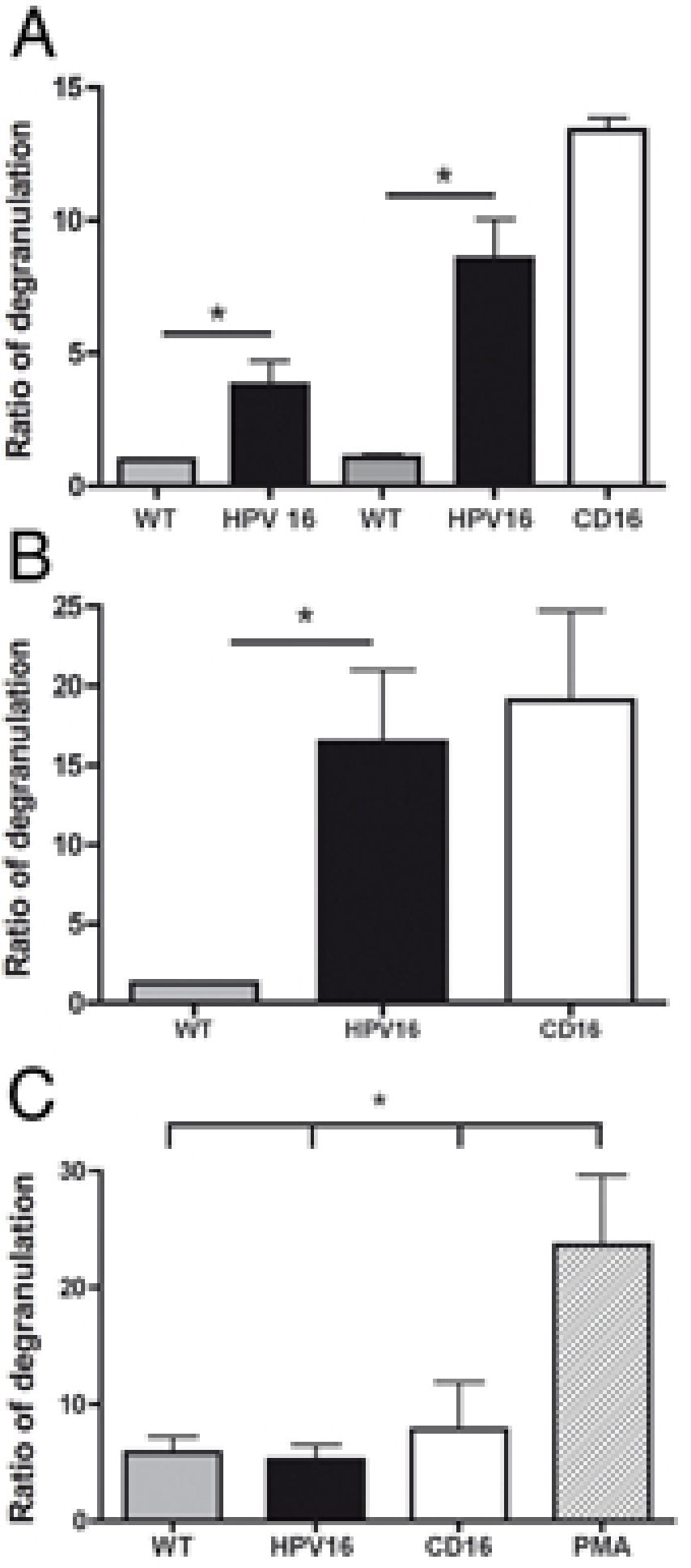
A
Ratio of degranulation
15
10
5
0
*
*
WT
HPV 16
WT
HPV16
CD16
B
Ratio of degranulation
25
20
15
10
5
0
*
WT
HPV16
CD16
C
Ratio of degranulation
30
20
10
0
*
WT
HPV16
CD16
PMA

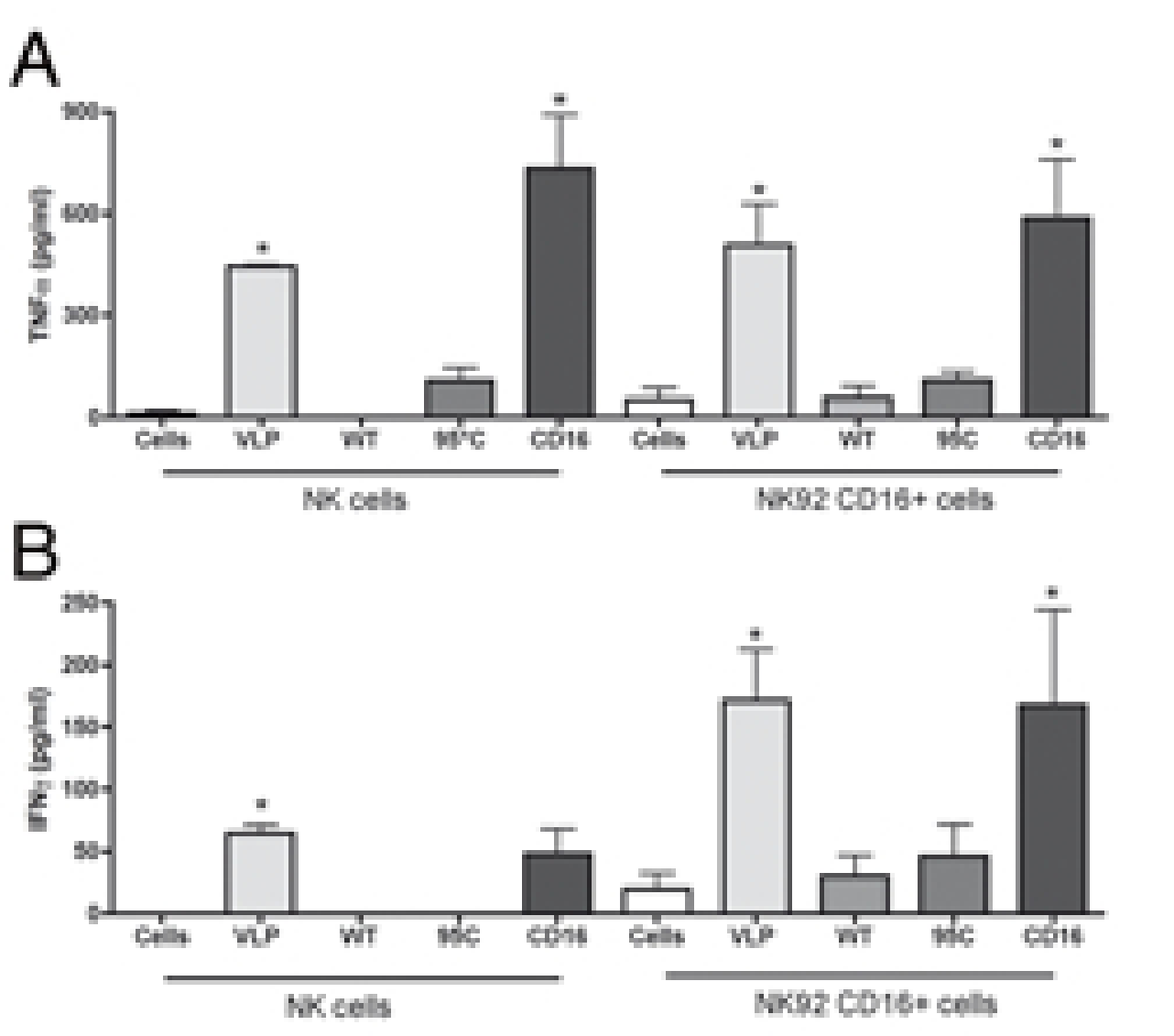
A
TNFα (pg/ml)
Cells
VLP
WT
95°C
CD16
Cells
VLP
WT
95C
CD16
NK cells
NK92 CD16+ cells
B
IFNγ (pg/ml)
Cells
VLP
WT
95C
CD16
Cells
VLP
WT
95C
CD16
NK cells
NK92 CD16+ cells